Generic Operational Characteristics of Piezoelectric Transformers

Gregory Ivensky, Isaac Zafrany, and Shmuel (Sam) Ben-Yaakov, *Member, IEEE*

***Abstract*—The universal attributes of piezoelectric transformers (PT) were derived by an approximate analysis that yielded closed form equations relating the normalized load resistance to the voltage gain, output power per unit and efficiency. Based on the results of the study, a calculation procedure is developed for specifying a PT for any given application and is demonstrated by considering the design of a fluorescent lamp driver. It is suggested that the closed form formulas, developed in this study, could be invaluable when studying, specifying and designing practical PTs applications.**

***Index Terms*—Approximate methods, fluorescent lamps, modeling, piezoelectric transformers, resonant power conversion.**

I. Introduction

PIEZOELECTRIC transformers (PT) have important advantages over low power electromagnetic (ferrite) transformers. In particular, they have high power density, small size and weight while maintaining high throughput efficiency. They could be designed to have very high voltage isolation between primary and secondary, can operate at high frequencies and they do not generate electromagnetic noise. Due to these advantages, PT have already found various practical applications [1]–[8] such as: electronic ballasts for fluorescent lamps, battery chargers for mobile phones, ac adapters for mobile computers, gate drives of MOSFETs and IGBTs and others.

Notwithstanding the fact that practical applications of PTs have been described in the literature, delineation of the engineering characterization of these devices is still insufficient [8]–[11]. For example, the PT analysis presented in [8], [9] was given only for the low voltage mode when the operating frequency is close to the series (i.e., mechanical) resonant frequency of PT. Operation in the high voltage mode provide maximum output voltage for a wide range of load resistances and could thus be useful in many applications. This mode was not analyzed in earlier publications. It should also be noted that the important functional relationship between the output power and load resistance was derived in [8], [9] for a relatively narrow range of load resistances. Consequently, it does not show the typical singularity of this function (two peaks of the output power). These and other issues were analyzed in this study and the theoretical results, verified by measurements and simulations, provide tools for evaluating the expected performance of a PT in a given application. Although this paper is concerned with PTs in ac–ac applications, the study can be used to assess the PT performance in converter applications (ac–dc) by applying the equivalent ac resistance approach (R_{ac}) [12] or the RC model for a converter with a capacitive filter [13], [14].

Manuscript received August 27, 2000; revised June 3, 2002. This work was presented at the Power Electronics Specialists Conference, Galway, Ireland, June 2000. Recommended by Associate Editor J. D. van Wyk.

The authors are with the Power Electronics Laboratory, Department of Electrical and Computer Engineering, Ben-Gurion University of the Negev, Beer-Sheva 84105, Israel (e-mail: sby@bguee.bgu.ac.il).

Digital Object Identifier 10.1109/TPEL.2002.805602

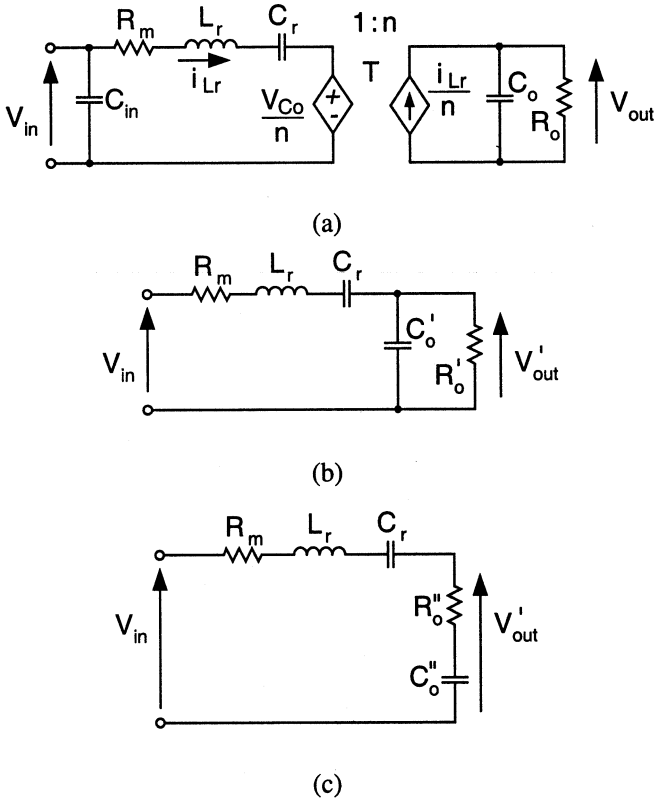

Fig. 1. Equivalent circuits of a piezoelectric transformer (PT): (a) general model, (b) after reflecting the output capacitance and load resistance to the primary, and (c) after parallel to series transformation.

II. Equivalent Circuits of Piezoelectric Transformers

The general equivalent circuit of a PT when operating around one of its mechanical resonant frequencies is depicted in Fig. 1(a). V_{in} and V_{out} are the input and output voltages, C_{in} and C_o are capacitances of the input and output capacitor, L_r and C_r are series equivalent inductance and capacitance, R_m is equivalent mechanical resistance, R_o is the load resistance and n is the mechanical output transfer ratio. The output transformer T (shown in earlier papers) is replaced in Fig. 1(a) by two dependent sources: v_{Co}/n and i_{Lr}/n.

This presentation is valid even when the output is exposed to a dc voltage. The electromagnetic transformer presentation (used

0885-8993/02$17.00 © 2002 IEEE

by other authors) would be undesirable in such a case, especially when the equivalent circuit is studied by circuit simulation. This is due to the fact that the windings of an electromagnetic transformer represent a short circuit to dc voltage.

From the power-transfer point of view, the basic equivalent circuit can be simplified to that of Fig. 1(b) in which the network at the secondary is reflected to the primary. Note that the input capacitance [C_{in} of Fig. 1(a)] is eliminated in Fig. 1(b) since it does not affect the power transfer of the PT except for the ESR effect that is treated in Section VI below. The values of the reflected resistance (R'_o), reflected capacitance (C'_o) and reflected output voltage (V'_{out}) will be

$$R'_o = \frac{R_o}{n^2} \tag{1}$$

$$C'_o = n^2 C_o \tag{2}$$

$$V'_{out} = \frac{V_{out}}{n}. \tag{3}$$

Further simplification can be achieved by converting the parallel network R'_o, C'_o to a series network [Fig. 1(c)] in which the series resistance R''_o and series capacitance C''_o are defined as

$$R''_o = \frac{R'_o}{1 + (\omega C'_o R'_o)^2} \tag{4}$$

$$C''_o = C'_o \frac{1 + (\omega C'_o R'_o)^2}{(\omega C'_o R'_o)^2} \tag{5}$$

where ω is the operating frequency.

III. An Intuitive Analysis

Examination of the dependence of R''_o and C''_o on R'_o reveals some interesting and important features. As R'_o varies from 0 to ∞, R''_o varies from zero back to zero with a maximum R''_{om} at

$$R'_{om} = \frac{1}{\omega C'_o}. \tag{6}$$

On the other hand, over the entire range of R'_o, series capacitance C''_o varies from infinity back to the value of C'_o.

Based on this simple observation some general conclusions can already be drawn.

1) For a given reflected load R'_o, maximum output voltage will be obtained at the resonant frequency ω_m (Fig. 1)

$$\omega_m = \frac{1}{\sqrt{L_r C_{eq}}} \tag{7}$$

where C_{eq} is the series value of C_r and C''_o

$$C_{eq} = \frac{C_r C''_o}{C_r + C''_o}. \tag{8}$$

2) The range of the series resonant frequency is dictated by the range of C''_o

$$\omega_{rs} < \omega_m < \omega_{ro} \tag{9}$$

where ω_{rs} is the resonant frequency at short circuit ($R_o = 0$)

$$\omega_{rs} = \frac{1}{\sqrt{L_r C_r}} \tag{10}$$

and ω_{ro} is the series resonant frequency at open circuit ($R_o = \infty$)

$$\omega_{ro} = \frac{1}{\sqrt{L_r \frac{C_r C'_o}{C_r + C'_o}}}. \tag{11}$$

3) For any given load (R_o), the output voltage can be controlled by shifting the frequency above or below ω_m. This is, in fact, the method used in inverters and converters operating in frequency-shift control mode.
4) For any given load (R_o), the fraction of power transferred to the load at the resonant frequency will depend on the ratio of R''_o to R_m [Fig. 1(c)].
5) Maximum power will be delivered to the load when $R''_o = R_m$. Since R''_o is convex, two R'_o (and hence two R_o) satisfy the maximum power condition.
6) At maximum output power ($R''_o = R_m$) the PT efficiency will be 0.5.
7) Maximum efficiency is obtained at the peak of R''_o.
8) Since maximum efficiency point corresponds to the maximum R''_o it also corresponds to a local minimum of output power (per a given input voltage).

IV. Detailed Analysis

A. Operating Frequency and Output to Input Voltage Ratio

The output to input voltage ratio k_{21} (Fig. 1) was found to be

$$k_{21} = \frac{V'_{out}}{V_{in}} = \frac{1}{\sqrt{Y}} \tag{12}$$

where

$$Y = \left\{1 - c\left[\left(\frac{\omega}{\omega_{rs}}\right)^2 - 1\right] + \frac{R_m}{R'_o}\right\}^2 + \left\{\frac{\omega_{rs}}{\omega}\frac{c}{Q}\left[\left(\frac{\omega}{\omega_{rs}}\right)^2 - 1\right] + \frac{\omega}{\omega_{rs}}\frac{c}{Q_m}\right\}^2 \tag{13}$$

$$c = \frac{C'_o}{C_r} \tag{14}$$

$$Q = \omega_{rs} C_o R_o \tag{15}$$

$$Q_m = \frac{1}{\omega_{rs} C_r R_m}. \tag{16}$$

Q is the electrical quality factor and Q_m is the mechanical quality factor.

Equation (12) implies that k_{21}has a maximum value (k_{21m}) when Y has a minimum value. Therefore, the frequency ratio ω_m/ω_{rs} corresponding to k_{21m} can be found by setting the derivative of the function (13) to zero. This was carried out two ways: by an exact and by an approximate analysis.

Exact analysis was based on the solution of the derivative of the third order equation (13), which can be presented by the canonical form

$$x^3 + \left[\frac{1}{2Q^2} + \frac{1}{2Q_m^2} - 1 - \frac{1}{c}\right]x^2 - \frac{1}{2Q^2} = 0 \tag{17}$$

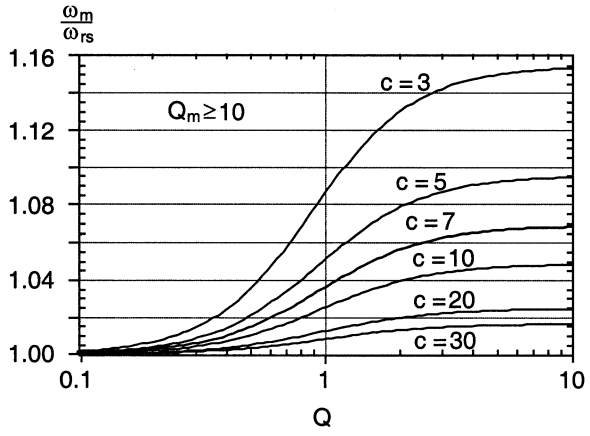

Fig. 2. Normalized operating frequency ω_m corresponding to the maximum output to input voltage ratio as a function of the electrical quality factor Q and capacitance ratio c for mechanical quality factor $Q_m \geq 10$ (ω_{rs} is the resonant frequency in short circuit mode).

where

$$x = \left(\frac{\omega_m}{\omega_{rs}}\right)^2. \tag{18}$$

The frequency ratio ω_m/ω_{rs} corresponding to the maximum value of $k_{21}(k_{21m})$, as a function of Q, Q_m and c, was found from (17) and (18) applying the "Mathematica" software package [15]. This dependence is plotted in Fig. 2. It shows that an increase of Q from zero to infinity shifts $\omega_m$from ω_{rs} to ω_{ro} as expected. The curves are valid for a large range of Q_m (10 to 1000). By inserting the values of ω_m/ω_{rs} into (13) and applying (12) we found the relationships between k_{21m} and circuit parameters Q, Q_m and c (Fig. 3).

The results of the exact analysis are based on numerical calculations and are therefore presented by tables and graphs. The results of the approximate analysis given below are presented in closed form equations and hence could be more convenient for design procedures. The approximation is based on the fact that the derivatives of some terms in (17) with respect to x are smaller than others and hence could be considered constant.

Taking into account the fact that near resonance the term $\{(\omega/\omega_{rs})^2 - 1\}$ is changing much more rapidly as a function of (ω/ω_{rs}) than does (ω/ω_{rs}), we replace here the first order multipliers (ω/ω_{rs}) and (ω_{rs}/ω) in (13) by as yet unknown constants

$$g = \frac{\omega}{\omega_{rs}} \quad \text{and} \quad \frac{1}{g} = \frac{\omega_{rs}}{\omega}. \tag{19}$$

Hence, (13) can be transformed into

$$Y = \left\{1 - c\left[\left(\frac{\omega}{\omega_{rs}}\right)^2 - 1\right] + \frac{R_m}{R'_o}\right\}^2 + \left\{\frac{c}{gQ}\left[\left(\frac{\omega}{\omega_{rs}}\right)^2 - 1\right] + \frac{gc}{Q_m}\right\}^2. \tag{20}$$

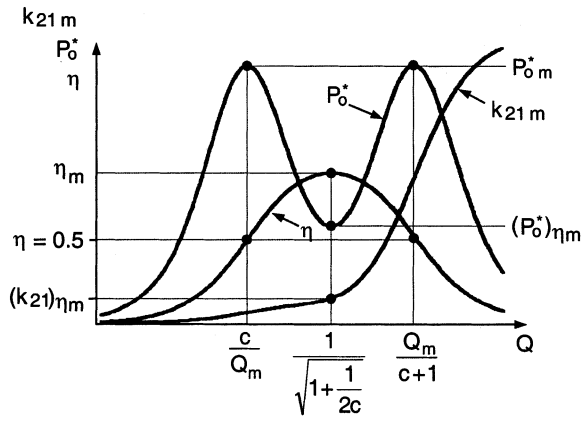

Fig. 3. Maximum value of the output to input voltage ratio k_{21m}, output power in per unit system P_o^* and efficiency η as a function of the electrical quality factor Q for c = const and Q_m = const.

Taking the derivative of (20) and equating it to zero, we solved the equation for the frequency ratio ω_m/ω_{rs}, corresponding to the maximum value of output to input voltage ratio k_{21m}

$$\frac{\omega_m}{\omega_{rs}} = \sqrt{1 + \frac{C_r}{C'_o}\frac{\left(\frac{\omega_m}{\omega_{rs}}\right)^2 Q^2}{1 + \left(\frac{\omega_m}{\omega_{rs}}\right)^2 Q^2}} = \sqrt{1 + \frac{C_r}{C'_o}\sin^2\varphi_m} \tag{21}$$

where φ_m is the phase angle of the parallel circuit $R'_oC'_o$ [Fig. 1(b)] at the frequency ω_m corresponding to the maximum value of the output to input voltage ratio k_{21m}

$$\varphi_m = \tan^{-1}\left(Q\frac{\omega_m}{\omega_{rs}}\right) = \tan^{-1}(\omega_m C'_o R'_o). \tag{22}$$

Applying (14) we derive from (21) the expression of ω_m/ω_{rs} in a form convenient for calculation

$$\frac{\omega_m}{\omega_{rs}} = \sqrt{0.5\left(1 + \frac{1}{c} - \frac{1}{Q^2}\right) + \sqrt{0.25\left(1 + \frac{1}{c} - \frac{1}{Q^2}\right)^2 + \frac{1}{Q^2}}}. \tag{23}$$

Note that the values of ω_m/ω_{rs} obtained by the approximate analysis are independent of R_m/R'_o [the terms including R_m/R'_o in (20) were reduced during the mathematical transformation].

By inserting (22) into (13) and applying (12), (14)–(16) and (22), we present a convenient expression for calculating the maximum value of the output to input voltage transfer ratio k_{21m}

$$k_{21m} = \frac{1}{\cos\varphi_m + \frac{R_m}{R_o\cos\varphi_m}} = \frac{1}{\cos\varphi_m + \frac{c}{Q_m Q\cos\varphi_m}}. \tag{24}$$

An approximate expression of k_{21m} under no load condition is obtained from (13) and (23)

$$(k_{21m})_{noload} = \frac{Q_m}{c\sqrt{1 + \frac{1}{c}}}. \tag{25}$$

Detailed comparison between simulation, exact analysis and approximate formulas for Q in the range of 0.01–100, Q_m in the range of 10–1000 and c in the range 0.5–50 reveal that the maximum discrepancy is smaller than 4.5%. In most operational regions, however, the agreement was found to be better than 0.1%. We believe therefore that the approximate (closed form) equations derived in this study are more than sufficient from the engineering point of view.

B. Output Power and Efficiency

The output power P_o can be calculated from

$$P_o = \frac{(k_{21m}V_{in})^2}{R_o} \tag{26}$$

or in per unit system [taking into account [(14) and (15)]

$$P_o^* = \frac{P_o}{P_{bas}} = \frac{ck_{21m}^2}{Q} \tag{27}$$

where P_{bas} is the base power unit

$$P_{bas} = V_{in}^2\sqrt{C_r/L_r}. \tag{28}$$

Efficiency can be found from [11]

$$\eta = \frac{R_o''}{R_o'' + R_m} \tag{29}$$

where R_o'' is the reflected load resistance in the equivalent series circuit $R_o''C_o''$ [Fig. 1(c)].

Applying (4) and (14)–(16) we transform (29) to obtain the expression for η in a form that is convenient for calculation

$$\eta = \frac{1}{1 + \frac{c}{Q_m}\left[\frac{1}{Q} + \left(\frac{\omega}{\omega_{rs}}\right)^2 Q\right]}. \tag{30}$$

The values of P_o^* and η, calculated from (27) and (30) as a function of the electrical quality factor Q for c = const and Q_m = const, are plotted in Fig. 3. These graphs reveal three extremes. Two of them correspond to the equal-height peaks of the output power $P_o^* = P_{om}^*$. The third extreme point corresponds to the maximum efficiency η_m and a local minimum per unit output power $(P_o^*)_{\eta_m}$.

To derive the location of these extreme points we find first the relationship between the output power P_o^* and efficiency η. Applying equations (27) and (29) of P_o^* and η and taking into account (4), (22) and (24) we obtain

$$P_o^* = \frac{c}{Q}\frac{1 + Q^2\left(\frac{\omega_m}{\omega_{rs}}\right)^2}{1 + \frac{2R_m}{R_o''} + \left(\frac{R_m}{R_o''}\right)^2} \tag{31}$$

$$\frac{R_m}{R_o''} = \frac{1}{\eta} - 1 \tag{32}$$

from which

$$\frac{P_o^*}{\eta^2} = c\left[\frac{1}{Q} + Q\left(\frac{\omega_m}{\omega_{rs}}\right)^2\right]. \tag{33}$$

Inserting (33) into (30) we find (Fig. 4)

$$\frac{P_o^*}{Q_m} = \eta(1-\eta). \tag{34}$$

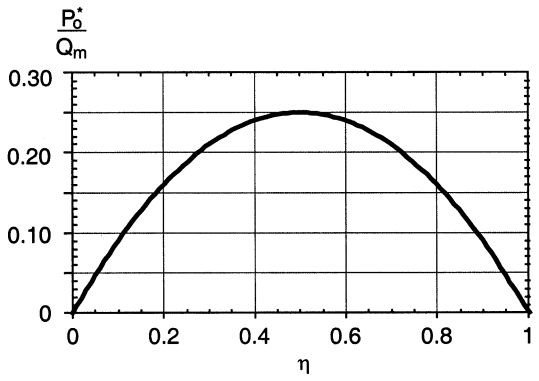

Fig. 4. Output power in per unit system P_o^* as a function of the efficiency η (Q_m is the mechanical quality factor).

It is clear that maximum output power P_{om}^* corresponds to the efficiency $\eta = 0.5$ and hence

$$P_{om}^* \approx 0.25Q_m. \tag{35}$$

Inserting $\eta = 0.5$ into (30) we find the following equation for the power peak points:

$$Q^2 - \frac{Q_m}{c\left(\frac{\omega_m}{\omega_{rs}}\right)^2}Q + \frac{1}{\left(\frac{\omega_m}{\omega_{rs}}\right)^2} = 0. \tag{36}$$

This equation has two solutions

$$Q_1 = \frac{1}{\frac{Q_m}{2c} + \sqrt{\left(\frac{Q_m}{2c}\right)^2 - \left(\frac{\omega_m}{\omega_{rs}}\right)^2}} \tag{37}$$

$$Q_2 = \left[\frac{Q_m}{2c} + \sqrt{\left(\frac{Q_m}{2c}\right)^2 - \left(\frac{\omega_m}{\omega_{rs}}\right)^2}\right]\left(\frac{\omega_{rs}}{\omega_m}\right). \tag{38}$$

We simplify these solutions taking into account the following conditions:

— $(Q_m/2c)^2$ is usually much larger than $(\omega_m/\omega_{rs})^2$;

— the value of Q_2 is practically very large and therefore $(\omega_m/\omega_{rs})^2 \approx 1 + (1/c)$ [see (21) and Fig. 2].

Under these conditions we obtain

$$Q_1 \approx \frac{c}{Q_m} \tag{39}$$

$$Q_2 \approx \frac{Q_m}{c+1}. \tag{40}$$

Now we consider the extreme point corresponding to the maximum value of the efficiency η_m. Analysis of (30) shows that $\eta = \eta_m$ when

$$Q\frac{\omega_m}{\omega_{rs}} = 1 \tag{41}$$

i.e., when $\varphi_m = \pi/4$ [see (22)]. The values of ω_m/ω_{rs} and Q corresponding to $\eta_m$are defined from (21) and (41)

$$\frac{\omega_m}{\omega_{rs}} = \sqrt{1 + \frac{1}{2c}} \tag{42}$$

$$Q = \frac{1}{\sqrt{1 + \frac{1}{2c}}}. \tag{43}$$

Inserting (42) and (43) into (30) we obtain the expression of the maximum efficiency

$$\eta_m = \frac{1}{1 + \frac{2c}{Q_m}\sqrt{1+\frac{1}{2c}}}. \tag{44}$$

Inserting (44) into (34) we obtain the output power at the point corresponding to the maximum value of the efficiency η_m

$$(P_o^*)_{\eta_m} = \frac{2c\sqrt{1+\frac{1}{2c}}}{\left(1+\frac{2c\sqrt{1+\frac{1}{2c}}}{Q_m}\right)^2}. \tag{45}$$

In the case that $Q_m \gg 2c$ the equation can be simplified to

$$(P_o^*)_{\eta_m} \approx 2c\sqrt{1+\frac{1}{2c}}. \tag{46}$$

C. Output to Input Voltage Ratio and Efficiency

Dependence between the output to input voltage ratio k_{21m} and efficiency η is found in the same manner as above. From (22) and (24) we define

$$k_{21m} = \frac{\sqrt{1+\left(Q\frac{\omega_m}{\omega_{rs}}\right)^2}}{1+\frac{c}{Q_m Q}\left[1+\left(Q\frac{\omega_m}{\omega_{rs}}\right)^2\right]}. \tag{47}$$

Inserting (47) into (30) we obtain

$$\eta = \frac{k_{21m}}{\sqrt{1+\left(Q\frac{\omega_m}{\omega_{rs}}\right)^2}}. \tag{48}$$

The value of k_{21m} corresponding to the efficiency peak point ($\eta = \eta_m$), defined as $(k_{21m})_{\eta_m}$, is found from (41) and (48)

$$(k_{21m})_{\eta_m} = \sqrt{2}\,\eta_m \tag{49}$$

or taking into account (44)

$$(k_{21m})_{\eta_m} \approx \frac{\sqrt{2}}{1+\frac{2c\sqrt{1+\frac{1}{2c}}}{Q_m}}. \tag{50}$$

V. PT With a Matching Inductor Connected in Parallel to the Output Terminals

The current of the output capacitance C_o [Fig. 1(a)] is lowering the efficiency since it passes through R_m. Hence, the overall efficiency of a PT can be improved by compensating the reactive current of C_o by an inductor L_{mt} connected in parallel to the output terminals of PT (Fig. 5).

For a perfect compensation

$$L_{mt} = \frac{1}{\omega^2 C_o} \tag{51}$$

where $\omega = \omega_{rs}$ is the operating frequency. The losses in the resistor R_m are lower in this case and therefore the efficiency of PT will be higher. In such a case, the equivalent resistances R_o'' and R_o' [Fig. 1(c) and (b)] have identical values and hence equation (29) of the PT efficiency is reduced to a following form:

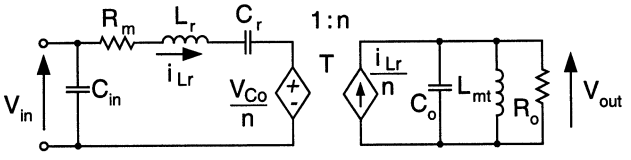

Fig. 5. Connection of a matching inductor L_{mt} in parallel to the output terminals of PT.

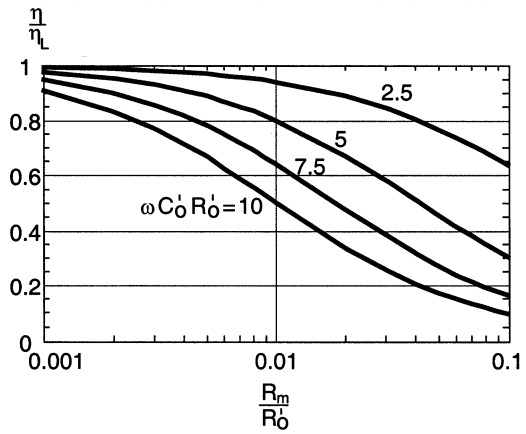

Fig. 6. Ratio of efficiency values expected without a matching inductor $L_{mt}(\eta)$ to the efficiency with an inductor (η_L) as a function of R_m/R_o' and $\omega C_o' R_o'$.

$$\eta_L = \frac{1}{1+\frac{R_m}{R_o'}}. \tag{52}$$

The ratio between the efficiency values in the two cases: without and with the matching inductor L_{mt} (η and η_L) is found from (52), (29) and (4)

$$\frac{\eta}{\eta_L} = \frac{1+\frac{R_m}{R_o'}}{1+\frac{R_m}{R_o'}\left[1+(\omega C_o' R_o')^2\right]} = \frac{1}{1+\frac{(\omega C_o' R_o')^2}{1+\frac{R_o'}{R_m}}}. \tag{53}$$

This relationship is shown in Fig. 6. We see that in general $\eta < \eta_L$ but for small R_m/R_o' and $\omega C_o' R_o'$ values, we find $\eta \approx \eta_L$

It should be noted that the matching inductor L_{mt}, operating in the resonant mode with C_o, decreases the output to input voltage transfer ratio k_{21m}

$$(k_{21m})_L \approx \eta_L. \tag{54}$$

To conserve the same output voltage V_{out}, input voltage V_{in} of PT must be increased.

VI. The Effect of the ESR of the Input and Output Capacitors

A modified equivalent circuit of a PT, taking into account the losses in the input and output capacitors C_{in} and C_o, is presented at Fig. 7(a). It includes parallel resistances $R_{Cin.par}$ and

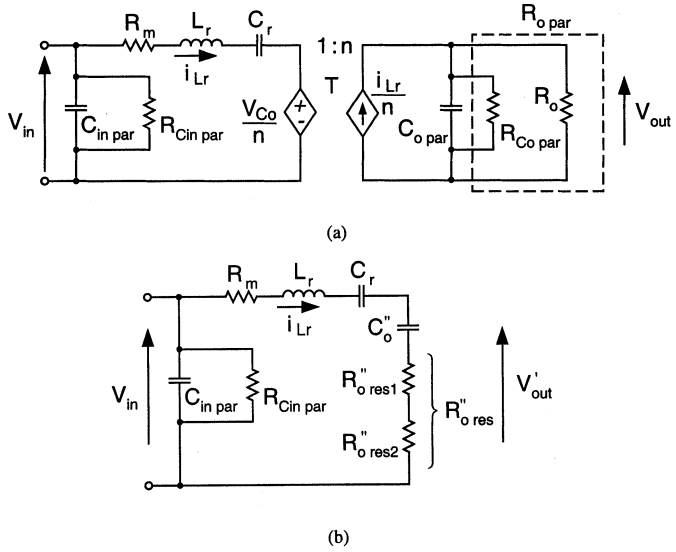

Fig. 7. Equivalent circuits of a piezoelectric transformer (PT) taking into account ESR losses in the input and output capacitors: (a) general model; (b) after reflecting the parameters of the secondary circuit to the primary and followed by a parallel to series transformation; $C_{in.par} \approx C_{in}; C_{o.par} \approx C_o$.

$R_{Co.par}$ which can be found from the following approximate equations:

$$R_{Cin.par} \approx \frac{1}{(\omega C_{in})^2 R_{Cin.ser}} \tag{55}$$

$$R_{Co.par} \approx \frac{1}{(\omega C_o)^2 R_{Co.ser}} \tag{56}$$

where $R_{Cin.ser}$ is the equivalent series resistance (ESR) of C_{in} and $R_{Co.ser}$ is the ESR of C_o. Hence, the losses in the input and output capacitors can be expressed as

$$P_{Cin} = \frac{V_{in}^2}{R_{Cin.par}} \tag{57}$$

$$P_{Co} = \frac{V_{out}^2}{R_{Co.par}} \tag{58}$$

where V_{in} and V_{out} are rms of the input and output voltage.

Due to $R_{Co.par}$, the total resistance $R_{o.res}$ at the output of the PT becomes smaller

$$R_{o.res} = \frac{R_o R_{Co.par}}{R_o + R_{Co.par}}. \tag{59}$$

Inserting $R_{o.res}$ (instead of R_o) into (15) we find the new value of the quality factor Q, and after using the data of Figs. 2 and 3 we obtain new values of ω_m/ω_{rs} and k_{21m}. The corrected terms are only slightly different from the values of the ideal case when $R_{Co.par} = \infty$. The output power P_o is calculated as before from (26), but its value is a little lower due the decrease in k_{21m}.

To derive the expression for the corrected efficiency, we reflect $R_{o.res}$ and C_o to the primary

$$R'_{o.res} = \frac{R_{o.res}}{n^2}. \tag{60}$$

Next we convert the parallel network $R'_{o.res}$, $C'_{o.res}$ to a series network [Fig. 7(b)] and calculate the series resistance $R''_{o.res}$

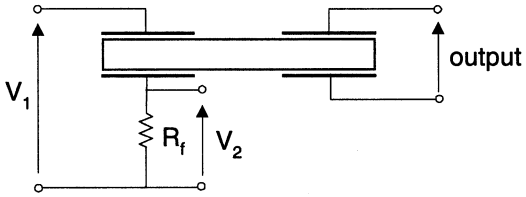

Fig. 8. Circuit connection when extracting PT parameters.

putting $R'_{o.res}$ [instead of R'_o] into (4). The resulting resistance $R''_{o.res}$ consists of two components connected in series

$$R''_{o.res1} = \frac{R''_{o.res}}{1 + \frac{R_o}{R_{Co.par}}} \tag{61}$$

$$R''_{o.res2} = \frac{R''_{o.res}}{1 + \frac{R_{Co.par}}{R_o}}. \tag{62}$$

The first component $(R''_{o.res1})$ is the equivalent load resistance while the second component $(R''_{o.res2})$ is the loss resistance of the capacitor C_o. If we neglect, at this stage, the losses in C_{in} we find the efficiency of a PT from the following equation:

$$\eta = \frac{R''_{o.res1}}{R''_{o.res} + R_m}. \tag{63}$$

Clearly, η_o is lower than in ideal case when $R_{Co.par} = \infty$.

Taking into account that the input capacitance C_{in} does not affect the power transfer of the PT we find the input power of a real PT applying (57) and (63)

$$P_{in} = \frac{P_o}{\eta_o} + \frac{V_{in}^2}{R_{Cin.par}}. \tag{64}$$

Hence, the efficiency of the PT including the losses due to the ESR of C_{in} will be

$$\eta = \frac{1}{\frac{1}{\eta_o} + \frac{V_{in}^2}{P_o R_{Cin.par}}}. \tag{65}$$

VII. Experimental

Philips piezoelectric transformer (RT 35 × 8 × 2 PXE43-S) with thickness polarization [11] was investigated experimentally. The values of the equivalent circuit components [Fig. 1(a)] were obtained by applying the circuit shown in Fig. 8 and with the help of a network analyzer (HP4395A). The outer shunt resistor R_f inserted in series with the PT input terminals is intended to sense the primary current of the PT when the output side is under short circuit conditions.

The parameters of the PT equivalent circuit [Fig. 1(a)] were extracted by applying the measurement method described below. The procedure assumes that $1/\omega_m C_{in} \gg R_m$ which is a good approximation for the PT under study. The dielectric capacitance C_{in} and C_o values are measured by a low frequency LCR meter.

The proposed procedure is based on two measurement sets: short and open circuit at the output of the PT. When the output is shorted, the resonant frequency ω_{rs} (10) is found and the

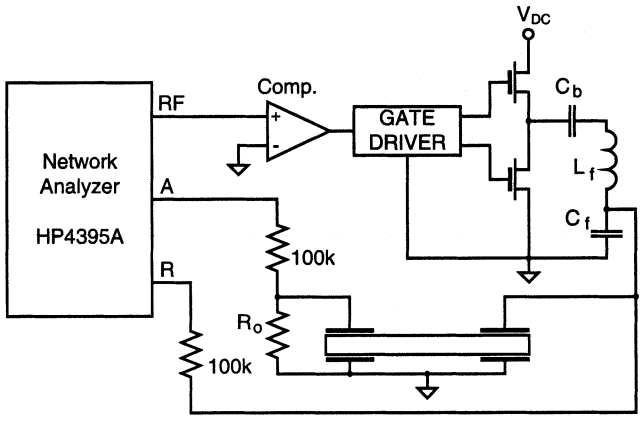

Fig. 9. Circuit diagram of the experimental setup.

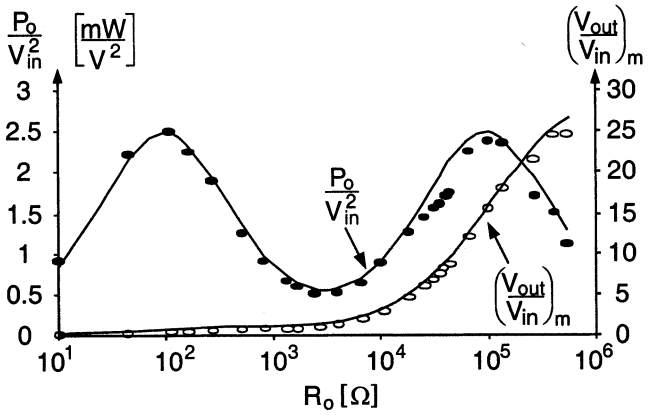

Fig. 10. Maximum value of the output to input voltage ratio $(V_{out}/V_{in})_m$ and the output power P_o as a function of the load resistance R_o: circles—experimental results; lines—theoretical prediction.

transfer function of V_2/V_1 (Fig. 8) at $\omega = \omega_{rs}$ is measured. Since this ratio is due to the voltage divider R_f, R_m

$$\frac{V_2}{V_1} = \frac{R_f}{R_f + R_m} \tag{66}$$

the equivalent mechanical resistance R_m can now be extracted. Next, by measuring the bandwidth (BW) around the series resonance peak, the mechanical quality factor Q_m is calculated

$$Q_m = \frac{f_{rs}}{\text{BW}} = \frac{\omega_{rs} L_r}{R_f + R_m} \tag{67}$$

L_r is computed from (67) and applying (10), C_r is extracted as well. Next, when the output is under open circuit condition, ω_{ro} (11) is measured and by substituting (2) into (11) the output transfer ratio n is calculated.

Applying the above procedure, the parameters of the experimental PT were found to be: $f_{rs} = \omega_{rs}/2\pi = 100.68$ kHz, $f_{ro} = \omega_{ro}/2\pi = 102.18$ kHz, $R_m = 100.5\ \Omega$, $L_r = 170$ mH, $C_r = 14.7$ pF, $C_{in} = C_o = 500$ pF and $n = 0.988$.

The circuit diagram of Fig. 9 was constructed and used to examine the input to output transfer function characteristic of the PT as a function of the load resistance R_o. A half bridge inverter was used to drive the primary of the PT and C_b, L_f and C_f filter was used to smooth the signal to an approximate sinusoidal waveform at the PT input terminals. This method could generate a high voltage sinusoidal signal at input terminal of the PT. The RF output of the network analyzer was used to feed the gate driver after passing a high-speed comparator to obtain a square wave signal. The transfer functions were measured by the A/R function of the analyzer (Fig. 9). It should be noted that the input impedance of A and R is 50 Ω and therefore series 100 kΩ resistors were used to avoid loading of the PT output and to reduce the signal level to the safe range for the analyzer. In this way, when the load resistance R_o was smaller then 100 kΩ the input to output transfer function was derived from V_A/V_R. For higher than 100 kΩ loads, the series resistances were replaced to higher values. Since the analyzer was calibrated with the series resistors (throughput), any error in the dividers was canceled out.

The experiments were carried out for a load resistance R_o range of 10 Ω to 540 kΩ. Each measurement point was taken at the frequency of maximum output voltage $V_{out.m}$. Excellent agreement was found between the experimental results and the corresponding values predicted by the equations derived in this study for the voltage gain and output power (Fig. 10).

VIII. Conclusion

The proposed method applies the equivalent circuit of the PT and the results are dependent on the values of the model parameters. It should be pointed out that PTs, in general, exhibit nonlinearity as well as temperature dependence. Consequently, the model parameters need to be extracted under the intended operating conditions. The experimental setup of Fig. 9 overcomes the output power imitation of common network analyzers by providing a synchronized high power driver to feed the PT. This solution is less costly than a high frequency high power amplifier that could be used, of course, for the same purpose. The narrow bandwidth of modern network analyzers, as the HP4395A, overcomes the distortion and hence a class D amplifier with a simple filter is sufficient for all practical purposes.

The generic equations developed in this study reveal some universal relationships between key parameters of a PT. These physical trade-offs can be used two ways: to optimize the design of a PT for a given application (see the Appendix) and/or specifying the desired PT to fill given tasks. From the engineering point of view it is clear that the range for high efficiency operation for a PT is:

$$\frac{c}{Q_m} < Q < \frac{Q_m}{c+1}. \tag{68}$$

Over this range the voltage transfer ratio is bound as follows:

$$0.5 < k_{21m} < \frac{0.5 Q_m}{\sqrt{c(c+1)}}. \tag{69}$$

Connection of a matching inductor L_{mt} in parallel to the output terminals of PT will increase the efficiency, but will decrease the output to input voltage ratio. The results displayed in Fig. 6 can be used to estimate the improvement in efficiency that can be gained by incorporating the compensating inductor. Trade-off between cost and performance can be examined.

As an example of the type of information that can be obtained by applying the results of this study, we considered in

the Appendix the case of a PT for fluorescent lamp drive. We assumed an 18 W lamp, driven by a PT that is fed by a 150 Vrms voltage (other specifications given in the Appendix). By applying the procedure outlined in the Appendix, we calculated the target PT parameters for this application. Obviously, many types of PT structures may comply with these target parameters, but once the desired parameters are defined, the search for the device is unequivocally defined. It is clear that at this stage of the PT technology, one may not be able to order a PT according to exact specifications. Even so, the required specifications, derived by above procedure, can help to select catalog products. The expressions developed in this study can then be applied to examine the expected performance when the available PT is used. It is thus concluded that the generic closed-form formulas, developed in this study, could be highly valuable when studying, specifying and designing practical PTs applications.

APPENDIX
SPECIFYING A PT FOR A FLUORESCENT LAMP

Similar to the case of electromagnetic transformers, the requirements of each application will dictate the parameters of the optimal PT. In the following we propose a method for specifying a PT used in a ballast for fluorescent lamps. The starting points of the design are: the nominal output power P_o, the input rms voltage V_{in}, the output rms voltage for the nominal load resistance (V_{out}) and under no load conditions ($V_{outnoload}$), the series resonant frequency ω_{rs}. For the nominal load resistance, the PT should operate in the extreme point of the characteristic (Fig. 3) corresponding to the maximum efficiency η_m; the value of η_m should also be specified.

Calculate:

1) The maximum value of the output to input voltage transfer ratio k_{21m}—eq. (49).

2) The transformer turn ratio "n" using (3) and (12):

$$n = \frac{V_{out}}{k_{21m} V_{in}}. \tag{70}$$

3) The capacitance ratio "c" using (25), (44) and (49):

$$c = \frac{h^2(1-\eta_m)^2 - 1}{2 - h^2(1-\eta_m)^2} \tag{71}$$

where

$$h = \frac{V_{outnoload}}{V_{out}} = \frac{k_{21mnoload}}{k_{21m}}. \tag{72}$$

4) The characteristic impedance of the series resonant circuit $\rho = \sqrt{L_r/C_r}$ using (27), (28), (44) and (45):

$$\rho = \frac{2V_{in}^2}{P_o}\,\eta_m^2 c\sqrt{1+\frac{1}{2c}}\,. \tag{73}$$

5) Inductance L_r and capacitance C_r:

$$L_r = \frac{\rho}{\omega_{rs}} \qquad C_r = \frac{1}{\omega_{rs}\rho}. \tag{74}$$

6) Capacitance C_o using (2) and (14):

$$C_o = \frac{c}{n^2}\,C_r. \tag{75}$$

7) The mechanical quality factor Q_m applying (44):

$$Q_m = \frac{\eta_m}{1-\eta_m}\,2c\sqrt{1+\frac{1}{2c}}\,. \tag{76}$$

8) Resistance R_m from (16):

$$R_m = \frac{\rho}{Q_m}. \tag{77}$$

Note that the equations of step 3) implies that $h(1-\eta_m)$ is bound:

$$1 < (1-\eta_m) < \sqrt{2}. \tag{78}$$

This limits should be taken into account in the beginning of the design when the values of "h" and η_m are specified.

As a numerical example, we consider the case of an 18 W lamp driven by a PT that is fed by a 150 Vrms source. The target specifications are assumed to be as follows: $P_{out} = 16$ W, $V_{out.nom} = 70$ Vrms, PT efficiency 90%, $f_{rs} = 100$ kHz.

To comply with (78), the parameter "h" was set to be $h = 14$. This corresponds to an open circuit voltage of 980 Vrms. In a practical application, a lower ignition voltage can be obtained by setting the operating frequency to be above the resonant frequency per (12), (13). Following the procedure outlined above, the target PT parameters for this application were calculated to be: $R_m = 126.5\ \Omega$, $L_r = 87.9$ mH, $C_r = 28.8$ pF, $C_o = 5.13$ nF, $n = 0.367$.

SPICE simulation was used to verify these numerical results. It was found that the calculated PT parameters meet the exact design requirements.

REFERENCES

[1] R. L. Lin, F. C. Lee, E. M. Baker, and D. Y. Chen, "Inductor-less piezoelectric transformer electronic ballast for linear fluorescent lamp," in *IEEE APEC'01 Rec.*, 2001, pp. 664–669.

[2] H. Kakedhashi, T. Hidaka, T. Ninomiya, M. Shoyama, H. Ogasawara, and Y. Ohta, "Electronic ballast using piezoelectric transformers for fluorescent lamps," in *IEEE PESC'98 Rec.*, pp. 29–35.

[3] Y. Fuda, K. Kumasaka, M. Katsuno, H. Sato, and Y. Ino, "Piezoelectric transformer for cold cathode fluorescent lamp inverter," *Jpn. J. Appl. Phys.*, pt. 1, vol. 36, no. 5B, pp. 3050–3052, May 1997.

[4] P. J. M. Smidt and J. L. Duarte, "Powering neon lamps through piezoelectric transformers," in *IEEE PESC'96 Rec.*, pp. 310–315.

[5] M. Imori, T. Taniguchi, H. Matsumoto, and T. Sakai, "A photomultiplier high voltage power supply incorporating a piezoelectric ceramic transformer," *IEEE Trans. Nucl. Sci.*, pt. 2, vol. 43, pp. 1427–1431, June 1996.

[6] T. Zaitsu, Y. Fuda, Y. Okabe, T. Ninomiya, S. Hamamura, and M. Katsuno, "New piezoelectric transformer converter for ac adapter," in *IEEE APEC'97 Rec.*, 1997, pp. 568–572.

[7] J. Navas, T. Bove, J. A. Cobos, F. Nuño, and K. Brebol, "Miniaturised battery charger using piezoelectric transformers," in *IEEE APEC'01 Rec.*, 2001, pp. 492–496.

[8] D. Vasic, F. Costa, and E. Sarraute, "A new MOSFET & IGBT gate drive insulated by a piezoelectric transformer," in *IEEE PESC'01 Rec.*, 2001, pp. 1479–1484.

[9] T. Zaitsu, T. Inoue, O. Ohnishi, and Y. Sasaki, "2 MHz power converter with piezoelectric ceramic transformer," *IEICE Trans. Electron.*, vol. E77-C, pp. 280–286, Feb. 1994.

[10] C. Y. Lin and F. C. Lee, "Design of a piezoelectric transformer converter and its matching networks," in *IEEE PESC'94 Rec.*, 1994, pp. 607–612.

[11] Philips, "Piezoelectric transformers," Application note Philips Magnetic Products, Date of release: 2/97.

[12] R. L. Steigerwald, "A comparison of half-bridge resonant converter topologies," *IEEE Trans. Power Electron.*, vol. 3, pp. 174–182, Apr. 1988.

[13] G. Ivensky, A. Kats, and S. Ben-Yaakov, "A RC-model of parallel and series-parallel resonant dc–dc converters with capacitive output filter," *IEEE Trans. Power Electron.*, vol. 14, pp. 515–521, May 1999.
[14] G. Ivensky, M. Shvartsas, and S. Ben-Yaakov, "Analysis and modeling of a piezoelectric transformer in high output voltage applications," in *IEEE APEC'00 Rec.*, 2000, pp. 1081–1087.
[15] S. Wolfram, *Mathematica. A System for Doing Mathematics by Computer*. Boston, MA: Addison-Wesley, 1988.

Gregory Ivensky was born in Leningrad, Russia, in 1927. He received the Energy Engineer Diploma from the Leningrad Railway Transport Institute in 1948 and the Candidate and Doctor of Technical Sciences degrees from the Leningrad Polytechnic Institute, in 1958 and 1977, respectively.

From 1951 to 1962, he was at the Central Design Bureau of Ultrasound and High Frequency Devices, Leningrad. From 1962 to 1989, he was at the Northwestern Polytechnic Institute, Leningrad, where in 1980 he became a Full Professor in the Department of Electronic Devices. Since 1991, he has been a Professor at the Department of Electrical and Computer Engineering, Ben-Gurion University of the Negev, Beer-Sheva, Israel. His research interests include rectifiers, inverters, dc–dc converters, EMI and power quality issues, and induction heating.

Isaac Zafrany was born in Ashqelon, Israel, in 1967. He received the B.Sc., M.Sc., and Ph.D. degrees in electrical and computer engineering from Ben-Gurion University of the Negev, Beer-Sheva, Israel, in 1993, 1996, and 2002, respectively.

His interests are in modeling and analysis of control of power electronic systems. He presently works in the field of electronic design automation (EDA) on analog circuit design issues at Avanti Corporation, Herzelia, Israel.

Shmuel (Sam) Ben-Yaakov (M'87) was born in Tel Aviv, Israel, in 1939. He received the B.Sc. degree in electrical engineering from the Technion, Haifa, Israel, in 1961 and the M.S. and Ph.D. degrees in engineering from the University of California, Los Angeles, in 1967 and 1970, respectively.

He is presently a Professor at the Department of Electrical and Computer Engineering, Ben-Gurion University of the Negev, Beer-Sheva, Israel, and heads the Power Electronics Group there. He served as the Chairman of that department, from 1985 to 1989. His current research interests include power electronics, circuits and systems, electronic instrumentation, and engineering education. He also serves as Chief Scientist of Green Power Technologies Ltd., Israel, and as a Consultant to commercial companies on various subjects, including analog circuit design and power electronics.